

# A W-band four-cavity gyrokystron amplifier

XU Shou-Xi<sup>1</sup>, LIU Pu-Kun<sup>1</sup>, ZHANG Shi-Chang<sup>1</sup>, XUE Qian-Zhong<sup>1</sup>, DU Chao-Hai<sup>1</sup>,  
GENG Zhi-Hui<sup>1</sup>, SU Yi-Nong<sup>1</sup>, LIU Gao-Feng<sup>1</sup>, SHI Shao-Hui<sup>1,2</sup>

(1. Key Laboratory of High Power Microwave Sources and Technologies, Institute of Electronics,  
Chinese Academy of Sciences, Beijing 100190, China;  
2. Department of Physics, Shijiazhuang University, Shijiazhuang 050035, China)

**Abstract:** The design of a W-band four-cavity gyrokystron amplifier is presented. The device operates in the fundamental harmonic TE<sub>01</sub> circular electric mode. The 70 kV, 6 A beam is produced by a double anode magnetron injection gun (MIG) with an average perpendicular-to-parallel velocity ratio of 1.5 and a parallel velocity spread of less than 4%. Particle-in-cell (PIC) simulations have been performed to predict general RF performance for various parameters. The simulated results show that the designed gyrokystron amplifier can produce about 35 dB gain, 800 MHz bandwidth and 100 kW peak output power with power conversion efficiency of 23.8% for a beam with 4% axial velocity spread.

**Key words:** Gyrokystron amplifier; magnetic injection gun (MIG); particle-in-cell (PIC) simulation

**PACS:** 84.40.Ik

## W 波段四腔回旋速调管放大器

徐寿喜<sup>1</sup>, 刘濮鲲<sup>1</sup>, 张世昌<sup>1</sup>, 薛谦忠<sup>1</sup>, 杜朝海<sup>1</sup>, 耿志辉<sup>1</sup>, 粟亦农<sup>1</sup>, 刘高峰<sup>1</sup>, 史少辉<sup>1,2</sup>

(1. 中国科学院电子学研究所 高功率微波源与技术重点实验室, 北京 100190;  
2. 石家庄学院 物理系, 河北 石家庄 050035)

**摘要:** 介绍了 W 波段四腔回旋速调管放大器的设计. 放大器工作在基膜 TE<sub>01</sub> 圆电模式, 电子束工作电压 70 kV, 工作电流 6 A, 设计的双阳极磁控式注入电子枪, 电子束纵横速度比 1.5, 速度零散小于 4%. 采用粒子模拟方法分析了各种参数对器件性能的影响. 模拟结果显示, 设计的放大器在电子束速度零散 4% 的情况下, 增益 35 dB, 带宽 800 MHz, 输出功率 100 kW, 效率为 23.8%.

**关键词:** 回旋速调管放大器; 磁控式注入电子枪; 粒子模拟

**中图分类号:** TN129 **文献标识码:** A

## Introduction

Gyrokystron amplifier based on electron cyclotron maser (ECM) mechanism can produce high power, high efficiency and satisfied bandwidth<sup>[1-3]</sup>. To date, gyrokystron amplifier is one of most practical power sources for millimeter wave radars in the atmospheric propagation windows around 35GHz and 94 GHz<sup>[4-5]</sup>.

In Russia, a two-cavity Ka-band gyrokystron produced pulsed output power of 750 kW at 35 GHz in the

TE<sub>021</sub> mode at 24% efficiency and 0.1% bandwidth<sup>[6]</sup>. A Ka-band second harmonic gyrokystron with permanent magnet has demonstrated a peak output power of 300 kW at 32.33 GHz with a 3-dB bandwidth of 40MHz, efficiency of 22%, and a saturated gain of 22 dB<sup>[7]</sup>. Two gyrokystrons with 500kW peak power and 1% duty factor have been used to drive a 34GHz radar system named RUZA<sup>[8]</sup>.

Likewise, in American, many advances have been made recently in the field of gyrokystron re-

**Received date:** 2012-04-27, **revised date:** 2012-12-30

**收稿日期:** 2012-04-27, **修回日期:** 2012-12-30

**Foundation items:** Supported by the National Natural Science Foundation of China (60971072, 61072024 and 61072026)

**Biography:** Xu Shou-xi (1971-), male, Laizhou, Shandong Province, China, Ph. D. Research fields include High Power Millimeter Wave Source and Technology. E-mail: xushouxi@mail.ie.ac.cn.

search. At the US Naval Research Laboratory (NRL), a two-cavity Ka-band gyrokystron amplifier has produced 210 kW peak power at 37% efficiency with 0.3% bandwidth<sup>[9]</sup>. A three-cavity design achieved power levels of 225 kW with 31% efficiency, 0.8% bandwidth, and 30-dB gain<sup>[10]</sup>. A W-band gyrokystron amplifier producing 10kW average power with a full-width at half-maximum (FWHM) bandwidth 600MHz has been developed for new high power radar named WARLOC<sup>[11-12]</sup>.

At the University of Maryland, researchers have developed X-band, Ku-band, and W-band gyrokystron amplifier for electron-positron collider applications<sup>[13-14]</sup>.

At the University of Electronic Science and Technology of China, a ka-band gyrokystron amplifier produced 300kW peak output power with 30% efficiency and 36dB gain<sup>[5]</sup>.

In the past, we investigated and conducted a prototype of a ka-Band second harmonic gyrokystron with 155MHz instantaneous bandwidth and 212kW output power<sup>[15]</sup>. The current paper presents the W-band high power gyrokystron amplifier planned to use in future millimeter wave radar applications. For this purpose the output power at least 100 kW are needed. The remainder of the paper is organized as follows. Section 2 presents the magnetron injection gun. The predicted characteristics simulated by PIC method are described in Section 3. The results are summarized and conclusions are drawn in Section 4.

**Table 1 Electron gun specifications and simulated performance**

**表 1 电子枪工作参数及模拟结果**

Beam voltage(kV)	70	Control anode voltage(kV)	23
Beam current(A)	6	Average velocity ratio	1.5
Emitter angle(deg)	50	Axial velocity spread (%)	3.5
Magnetic compression ratio	25		

## 1 Magnetron injection gun

A high quality electron optics system is critical to the successful operation of four-cavity gyrokystron amplifier. So the gun design is a key element in the design of gyrokystron amplifier. For gyrodevices, magnetron injection gun (MIG) have been the standard beam

forming system and proven to be effective. In our designed gyrokystron, a double anode MIG was employed. The EGUN code was used to simulate the performance of the electron gun. Fig. 1 gives the profile of the electron gun and beam trajectories. Table 1 lists the key parameters, while the gun performance is summarized in Fig. 2. It can be seen that for a beam current of 6 A, the velocity ratio ( $\alpha$ ) of 1.5 is achieved with a spread of 3.5% in the parallel velocities.

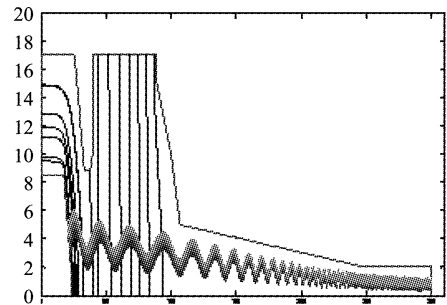


Fig. 1 Electron trajectory simulated by the E-gun code

图 1 E-gun 模拟的电子轨迹

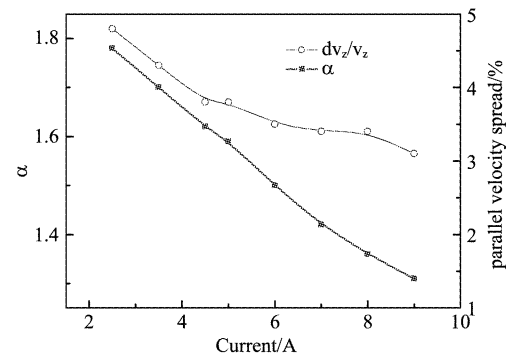


Fig. 2 The dependences of alpha and the velocity spreads on the beam current

图 2 电子注速度比和速度离散随电流的变化情况

## 2 Circuit design

One problem with W-band gyrokystron is a need for the available high power input power source. For this reason, it is important for gyrokystron amplifier with high gain. This requires a gyrokystron with 3 or more cavities. Our gyrokystron interaction circuit employed four cavities consisting of an input cavity, two bunching cavities and a final output cavity using stagger-tuning technology to achieve the desired gain, pow-

er and bandwidth. In order to achieve stable operation, the cavities are separated by drift tubes. The drift tubes are loaded with lossy ceramics to restrain adjacent cavities from coupling. The radii of drift tube were chosen to prevent  $TE_{01}$  mode propagation at the operating frequency.

CHIPIC is a highly efficient particle-in-cell code which is used to solve the high power microwave electromagnetic field problems<sup>[16]</sup>. Previously, we employed CHIPIC code to study a ka-band second harmonic gyrokystron amplifier; the simulation result was very good in agreement with the experiment test<sup>[17]</sup>. In this section, we used CHIPIC code to model the gyrokystron interaction circuit.

**Table 2** Cavity parameters of the designed four-cavity gyrokystron amplifier

表 2 四腔回旋速调管的腔体参数

Cavity	Length	Q factor	Frequency (GHz)
Input	$1.2\lambda$	165	94.39
Bunch	$1.6\lambda$	142	94.3
Penultimate	$1.6\lambda$	200	94.3
Output	$3\lambda$	100	94.0

The optimization of the interaction circuit for the gyrokystron amplifier is a complex and tradeoff process. Through the repeated adjustments using PIC simulation, the optimized circuit parameters of the W-band four-cavity gyrokystron amplifier are listed in Table 2. The radii of drift tubes were chosen to be  $6\lambda$ . In the following simulation, unless otherwise stated, the operating parameters in PIC simulation are given in table3.

Fig. 3 (a) gives the simulation model and the distribution of electric field in the circuit. From the graph, we can see that the operating mode is primary  $TE_{01}$  mode and the RF amplitude gradually strengthens along the  $z$ -axis. A Fourier transformed frequency spectrum of the electric field is given in Fig. 3(b). As shown in Fig. 3(b), a single frequency is observed at 94.5 GHz without any mode competition.

Fig. 4 gives the change of the relativistic factors along the  $z$  axis. From Fig. 4, we can see that the relativistic factors of all electrons slowly change from 1.137 until reaching the output cavity; in the output cavity, some electrons obtain the energy, their relativistic fac-

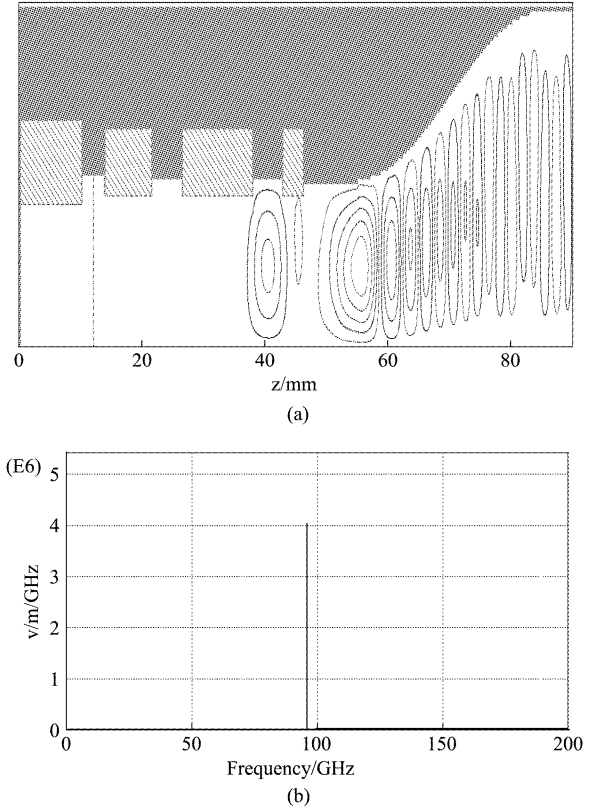


Fig. 3 (a) Simulation model and distribution of azimuthal electric field in the circuit. (b) A frequency spectrum obtained from Fourier transformation of the electric fields

图 3 (a) 相互作用电路物理模型及角向电场分布, (b) 傅里叶变化得到的电场频谱图

tors have increased, but most electrons lose the energy, their relativistic factors reduce, as is expected.

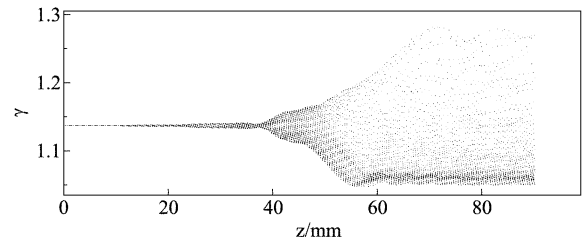


Fig. 4 The relativistic factors of the electrons along the  $z$  axis

图 4 电子的相对论因子沿  $z$  轴的变化情况

Fig. 5 gives the peak output power and gain versus input power for the circuit parameters at a drive frequency of 94.50 GHz under the assumption of an ideal electron beam. It is apparent that the output power rapidly increases with increasing input power when the input power is less than about 20W. However, the out-

put power slowly decreases with increasing input power when the input power surpasses 40W or so. On the contrary, the gain decreases monotonically with increasing input power. As shown in Fig. 5, the output power and gain reach maximums of 143 kW and 34% , respectively, at a drive power of 34 W , corresponding to a saturated gain of 36 dB.

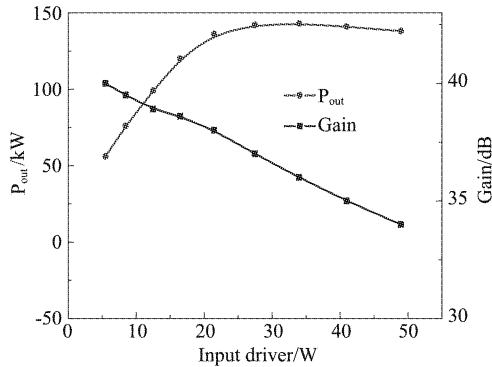


Fig. 5 Predicted dependence of the output power and efficiency on the input power for a 70 kV, 6 A electron beam with  $\alpha = 1.5$

图5 输出功率和效率随输入功率的变化情况 ( $U = 70$  kV,  $I = 6$  A,  $\alpha = 1.5$ )

Table 3 Operating parameters for the four-cavity gyrokylystron circuit

表3 四腔回旋速调管的工作参数

Voltage(kV)	70
Current (A)	6
Velocity ratio $\alpha$	1.5
Magnetic field(T)	3.6
Input power(W)	30
Operating mode	TE011
Cyclotron harmonic(s)	1

The dependence of efficiency on peak magnetic field is indicated in Fig. 6. As the magnetic field is varied, the beam voltage, beam current and drive power remained fixed. As shown in Fig. 6, the maximum efficiency is 34% when the applied magnetic field is 36kG.

The calculated output power is shown in Fig. 7 as a function of the frequency for various axial velocity spreads ( $dv_z/v_z$ ) of the electron beam. The output power drops rapidly as the beam velocity spread increase. When the axial spread increase to 4% , the output power drops from 143kW to 100kW at 94.6GHz. Accordingly, the 3dB bandwidth drops from 1GHz to 800MHz.

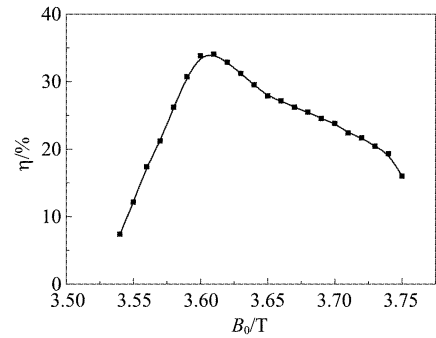


Fig. 6 The dependence of efficiency on magnetic field

图6 输出效率随磁场的变化情况

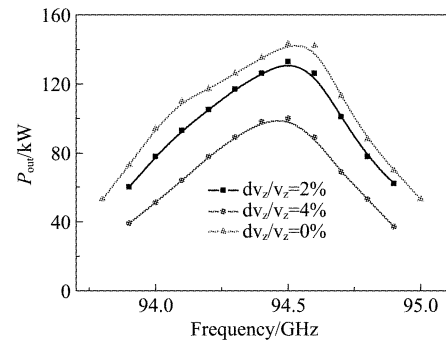


Fig. 7 The effect of the electron velocity spread on the bandwidth and the output power for a 70 kV, 6 A

图7 电子注的速度离散对带宽和输出功率的影响 ( $U = 70$  kV,  $I = 6$  A)

The input coupler is one of the key components of the amplifier due to strict requirements such as high mode purity and coupling efficiency. To meet these requirements, a coaxial input coupler is designed to couple power from the driver to the circuit. Fig. 8 shows the electric field distribution. We can see that the  $TE_{511}$  mode of the outer cavity is excited and the power is then magnetically coupled to the  $TE_{011}$  mode of the inner cavity through five axial slots spaced 72 degrees from each other in azimuth. The cut off drift tube has been included at both ends of the inner cylindrical cavity.

The output coupling waveguide is designed to connecting the output cavity up to collector. The Dolph-Chebyshev (D-C) taper turned out to be good performance with low mode conversion<sup>[18]</sup>. So we employed the D-C taper to minimize mode conversion. Fig. 9 gives the simulation results.

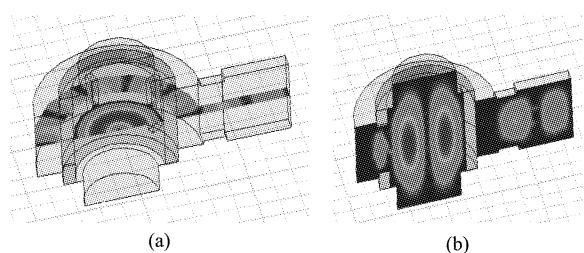


Fig. 8 (a) The distribution of electric field at an axial cut-plane. (b) The distribution of electric field at the transverse cut-plane

图 8 (a) 电场在轴切面的分布情况 (b) 电场在横切面上的分布情况

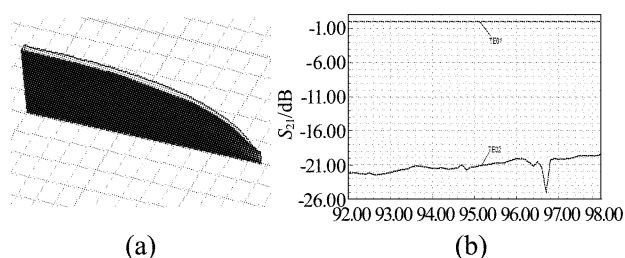


Fig. 9 (a) The distribution of electric field. (b) Transmission characteristic for operating mode  $TE_{01}$  and unwanted mode  $TE_{02}$

图 9 (a) 电场分布图 (b)  $TE_{01}$  模和  $TE_{02}$  模的传输特性

### 3 Conclusion

We have presented the design of a four-cavity, 94GHz gyrokystron. The gyrokystron amplifier operates stably in the fundamental harmonic  $TE_{01}$  circular cavity mode. A high quality double anode MIG was used. The effects of various parameters, such as input power, frequency, velocity spread and magnetic field on the electronic efficiency, gain, and output power were discussed. Simulations predict that the peak output power was 100kW at 94.5GHz corresponding to power conversion efficiency of 23.8%, when a 70kV, 6A annular electron beam with a perpendicular velocity to parallel velocity ratio of 1.5 was used. The 3dB instantaneous bandwidth is 800MHz for a beam with 4% axial velocity spread.

### REFERENCES

- [1] Barker R J, Schamiloglu E. *High-Power Microwave Sources and Technologies*[M]. Piscataway, NJ: IEEE, 2001.
- [2] Felch K L, Danly B G, Jory H R, *et al.* Characteristics and applications of fast-wave gyrodevices [J]. *Proc. IEEE*, 1999, **87**(5): 752 – 781.
- [3] Granatstein V L, Baruch Levush, Danly B G. *et al.* A quarter century of gyrotron research and development [J]. *IEEE Trans. Plasma Sci.*, 1997, **25**(6): 1322 – 1335.
- [4] Chu K R. The electron cyclotron maser [J]. *Rev. Modern Phys.* 2004, **76**(2), 489 – 540.
- [5] Thumm M. State-of-the-art of high power gyro-devices and free electron masers update 2011, KIT Scientific Reports 7606 [EB OL]. <http://uvka.ubka.uni-karlsruhe.de/shop/download>.
- [6] Antokov I I, Zasyplin E V, Sokolov E V. 35GHz radar gyrokystron [C]. in Proc. 18th Int. Conf. IR&MM Waves, UK, 1993: 338 – 339.
- [7] Gachev I G, Antakov I I, Lygin V K, *et al.* A ka-band second-harmonic gyrokystron with permanent magnet [C]. Fifth International Workshop Strong Microwaves in Plasmas, Russia, 2002.
- [8] Tolkachev A A, Solovjev B A, Solovjev G K. *et al.* A megawatt power millimeter-wave phase-array radar [J]. *IEEE AES Systems Magazine*, 2000, **7**: 25 – 31.
- [9] Choi J J, McCurdy A H, Wood F N, *et al.* Experimental investigation of a high power, two-cavity, 35GHz gyrokystron amplifier [J]. *IEEE Trans. Plasma Sci.*, 1998, **26**(3): 416 – 425.
- [10] Calame J P, Garven M, Choi J J, *et al.* Experimental studies of bandwidth and power production in a three-cavity, 35GHz gyrokystron amplifier [J]. *Phys. Plasma*, 1999, **6**(1): 285 – 297.
- [11] Ngo M, Danly B G, Myers R, *et al.* High-power millimeter-wave transmitter for the NRL WARLOC radar [C]. IVEC2002, USA: Monterey, 2002: 363 – 364.
- [12] Blank M, Danly B G, Levush B, *et al.* Demonstration of a 10 kW average power 94 GHz gyrokystron amplifier [J]. *Physics of plasmas*, 1999, **6**(12): 4405 – 4409.
- [13] Granatstein V L, Lawson W. Gyro-amplifiers as candidate RF drivers for TeV linear colliders [J]. *IEEE Trans. Plasma Sci.*, 1996, **24**(3): 648 – 665.
- [14] Lawson W, Cheng J, Calame J P, *et al.* High power operation of a three-cavity X-band coaxial gyrokystron [J]. *Phys. Rev. Lett.*, 1998, **81**, 3030 – 3033.
- [15] Liu Pu-Kun, Zhang Shi-Chang, Xu Shou-Xi, *et al.* Experimental studies of a ka-band second harmonic gyrokystron [C]. IRMMW-THz2010, Italy: Rome, 2010.
- [16] DI Jun, ZHU Da-Jun, LIU Sheng-Gang, Electromagnetic field algorithms of CHIPIC Code [J]. *Journal of UEST of China*, 2005, **34**(4), 485 – 488.
- [17] Liu Pu-Kun, Zhang Shi-Chang, Xu Shou-Xi, *et al.* Recent results in the development of a ka-band second harmonic gyrokystron amplifier [C]. IVEC2007, Japan, 2007, 237 – 238.
- [18] Heinrich FLÜGEL, Eberhard KÜHN, Computer-aided analysis and design of circular waveguide tapers [J]. *IEEE Trans. On MTT*, 1988, **36**(2), 332 – 336.